Table IV. Uv-Visible Absorption Bands ($cm^{-1} \times 10^{-3}$) of paphy, $[Yb(paphy)(H_2O)_3(OH)]_2Cl_4 \cdot 4H_2O$ (Complex A), and Dehydration Product (complex B), Recorded as Nujol Mulls

	Paphy	Complex A	Complex B
Band I	42.3	38.8	35.8
		32.1	31.8
Band II	29.9	27.2 (sh)	26.4 (sh)
		24.8 (sh)	21.8 (sh)

any magnetic interaction at temperatures above 220 K. Below this temperature there is a small deviation from Curie–Weiss behavior. The magnetic properties of the complex between 4 and 90 K are being studied further. In a chloro-bridged dimeric complex with a Yb–Yb separation of 3.98 Å, Raymond found no magnetic interaction between the Yb(III) atoms at temperatures down to 4 K.[23,24]

Ultraviolet–Visible Spectra. The solid-state uv–visible spectra of the free ligand, the complex, and the final dehydration product obtained after prolonged heating and the loss of four H_2O per Yb are summarized in Table IV. The spectrum of the free ligand has two strong bands. These bands split and undergo large bathochromic shifts when the ligand becomes coordinated to Yb(III). The bands move to even longer wavelengths in the dehydration product. The stepwise dehydration of the complex (see Experimental Section) is consistent with the initial loss of two molecules of lattice H_2O per Yb atom, followed by the loss of two coordinated H_2O molecules per Yb atom. A reduction of the coordination number of Yb from 8 to 6 would account for the large bathochromic shift on dehydration.

Acknowledgment. Financial support from the Australian Research Grants Committee (Grant 65/15552) and from the U.S. Public Health Service (Grant GM-10867) is gratefully acknowledged.

Registry No. A, 59738-47-5; B, 59738-48-6.

Supplementary Material Available: Listings of (i) the infrared spectroscopic data for paphy and $[Yb(paphy)(H_2O)_3(OH)]_2Cl_4 \cdot 4H_2O$ and (ii) the x-ray structure factor amplitudes for $[Yb(paphy)(H_2O)_3(OH)]Cl_2 \cdot 2H_2O$ in $[Yb(paphy)(H_2O)_3(OH)]_2Cl_4 \cdot 4H_2O$ (22 pages). Ordering information is given on any current masthead page.

References and Notes

(1) E. Baraniak and J. M. James, unpublished work.
(2) B. N. Figgis and J. Lewis, "Modern Coordination Chemistry", J. Lewis and R. G. Wilkins, Ed., Interscience, New York, N.Y., 1960, p 403.
(3) H. C. Freeman, J. M. Guss, C. E. Nockolds, R. Page, and A. Webster, *Acta Crystallogr., Sect. A*, **26**, 149 (1970).
(4) W. C. Hamilton, *Acta Crystallogr.*, **8**, 185 (1955).
(5) P. Coppens, L. Leiserowitz, and D. Rabinovich, *Acta Crystallogr.*, **18**, 1035 (1965).
(6) A. D. Rae, *Acta Crystallogr.*, **19**, 683 (1965); A. D. Rae and A. B. Blake, *ibid.*, **20**, 586 (1966).
(7) D. T. Cromer and J. T. Waber, *Acta Crystallogr.*, **18**, 104 (1965).
(8) D. T. Cromer, *Acta Crystallogr.*, **18**, 17 (1965).
(9) $R_1 = \sum||F_o| - s|F_c||/\sum|F_o|$; $R_2 = [\sum w||F_o| - s|F_c||^2/\sum w|F_o|^2]^{1/2}$.
(10) See paragraph regarding supplementary material.
(11) W. R. Busing, K. O. Martin, and H. A. Levy, Report ORNL-TM-305, Oak Ridge National Laboratory, Oak Ridge, Tenn., 1962.
(12) C. K. Johnson, Document ORNL-3794, Oak Ridge National Laboratory, Oak Ridge, Tenn., 1965.
(13) S. P. Sinha, "Structure and Bonding", Vol. 25, J. D. Dunitz et al., Ed., Springer, Berlin, 1975, p 69.
(14) J. L. Hoard and J. V. Silverton, *Inorg. Chem.*, **2**, 235 (1963).
(15) S. J. Lippard, *Prog. Inorg. Chem.*, **8**, 109 (1967).
(16) M. Gerloch, *J. Chem. Soc. A*, 1317 (1966).
(17) R. St. L. Bruce, M. K. Cooper, H. C. Freeman, and B. G. McGrath, *Inorg. Chem.*, **13**, 1032 (1974).
(18) Details and advantages of the method used to represent chelate ring conformations in Figure 4 are discussed by H. C. Freeman, M. J. Healy, and M. L. Scudder, *J. Biol. Chem.*, in press.
(19) C. F. Bell and D. R. Rose, *Inorg. Chem.*, **7**, 325 (1968).
(20) L. J. Basile, D. L. Gronert, and J. R. Ferraro, *Spectrochim. Acta, Part A*, **24**, 707 (1968).
(21) J. Ferraro, *Anal. Chem.*, **40**, 24A (1968).
(22) J. H. Van Vleck and A. Frank, *Phys. Rev.*, **34**, 1494 (1929).
(23) E. C. Baker, L. D. Brown, and K. N. Raymond, *Inorg. Chem.*, **14**, 1376 (1975).
(24) K. N. Raymond, personal communication.

Contribution from the Department of Chemistry, University of Iowa, Iowa City, Iowa 52242

Crystal and Molecular Structure of Bis[bis(diphenylethylphosphine)silver(I)] Bis(1,2-dicyano-1,2-ethylenedithiolato)nickelate(II), $[Ag(P(C_6H_5)_2(C_2H_5))_2]_2Ni(S_2C_2(CN)_2)_2$. Steric Effects on the P–Ag–P Angle

F. J. HOLLANDER, Y. L. IP, and D. COUCOUVANIS*

Received February 19, 1976 AIC60134V

Bis[bis(diphenylethylphosphine)silver(I)] bis(1,2-dicyano-1,2-ethylenedithiolato)nickelate(II), $[Ag(P(C_6H_5)_2(C_2H_5))_2]_2Ni(S_2C_2(CN)_2)_2$, crystallizes in the orthorhombic space group *Pbca* with four molecules per unit cell. The cell dimensions are $a = 18.427$ (9) Å, $b = 26.894$ (10) Å, and $c = 13.149$ (9) Å. Intensity data were collected with a four-circle computer-controlled diffractometer using the θ–2θ scan technique. All 40 nonhydrogen atoms were refined anisotropically and the 30 hydrogen atoms were included as fixed atoms. Refinement by full-matrix least squares using 2113 reflections gave an R value of 0.023 for 358 parameters. The geometry of the NiS_4 group is square planar. The interaction of $Ag(PPh_3)_2^+$ occurs at the NiS_4 group and the silver atoms are located above and below the NiS_4 plane in a chair configuration. Average values of selected bond distances and angles in the $(AgP_2)_2NiS_4$ core are as follows: Ag–Ni = 2.986 Å, Ag–S = 2.854 Å, Ni–S = 2.177 Å, Ag–P = 2.449 Å, Ni–Ag–S = 43.70°, S–Ni–S(interligand) = 87.55°, S–Ni–S(intraligand) = 92.45°, P–Ag–P = 128.00°. The ^{31}P NMR spectra of the $[(P(C_6H_5)_n(C_2H_5)_{3-n})_2Ag]_2Ni(mnt)_2$ complexes ($n = 0, 1, 2, 3$) were obtained and the ^{107}Ag–^{31}P coupling constants were 394, 413, 426, and 426 Hz for $n = 3$, 2, 1, and 0, respectively. These data when correlated to P–Ag–P angle values indicate the importance of steric effects in determining the s character of the Ag–P bond.

Introduction

In a recent study of the solution structure of silver(I)–phosphine complexes, Muetterties and Alegranti[1] presented some interesting conclusions about the structural and kinetic features of these compounds. A notable characteristic in the ^{31}P nuclear magnetic resonance spectra of the $((tol)_3P)_2AgL$ complexes was the variation in magnitude of the Ag–^{31}P coupling constants. Thus values from 380 to 470 Hz were observed in compounds for which conductivity studies did not indicate an appreciable extent of dissociation (eq 1).

$$(P(tol)_3)_2AgL \rightleftarrows (P(tol)_3)_2Ag^+ + L^- \quad (1)$$

The values of the Ag–P coupling constant, to a first approximation, can be correlated with the percent s character

Table I. Final Positional and Thermal Parameters for the Atoms in $[Ag(PPh_2Et)_2]_2Ni(mnt)_2$[a]

ATOM	X	Y	Z	B11	B22	B33	B12	B13	B23
NI	0	0	0	3.70(4)	3.92(4)	5.32(4)	-0.36(3)	-0.32(3)	-0.59(3)
AG	0.02300(2)	0.10234(1)	0.08202(2)	4.14(2)	4.29(2)	5.62(2)	-0.29(1)	0.55(1)	-1.05(2)
P(1)	-0.03287(6)	0.15030(4)	0.22061(8)	3.96(6)	3.70(6)	5.10(6)	-0.13(5)	0.76(5)	-0.41(5)
P(2)	0.14623(6)	0.10904(4)	0.01580(9)	3.94(5)	3.94(7)	4.73(6)	-0.21(5)	0.41(5)	-0.48(5)
S(1)	-0.00597(6)	0.00318(5)	0.16516(9)	4.97(6)	4.65(7)	5.49(6)	-0.33(5)	-0.09(5)	-0.43(5)
S(2)	0.09228(6)	-0.05054(5)	0.0035(1)	4.08(5)	4.96(7)	6.47(7)	0.14(5)	-0.72(5)	-1.07(6)
N(1)	0.0854(3)	-0.0447(2)	0.3942(4)	12.4(4)	9.5(4)	7.0(3)	-1.7(3)	-2.1(3)	1.3(3)
N(2)	0.2128(3)	-0.1164(2)	0.1830(4)	6.0(3)	6.5(3)	12.4(4)	0.5(2)	-2.7(2)	0.2(3)
C(1)	0.0648(3)	-0.0347(2)	0.2020(4)	5.6(3)	3.7(3)	5.3(3)	-1.3(2)	-1.4(2)	-0.0(2)
C(2)	0.0772(3)	-0.0403(2)	0.3084(5)	7.2(3)	5.1(3)	7.2(4)	-1.2(2)	-0.9(3)	0.5(3)
C(3)	0.1072(3)	-0.0586(2)	0.1326(4)	4.5(2)	3.4(3)	7.1(3)	-0.6(2)	-1.6(2)	-0.8(2)
C(4)	0.1662(3)	-0.0902(2)	0.1619(4)	5.2(3)	4.3(3)	9.0(4)	-0.7(3)	-1.5(3)	-0.5(3)
C(5)	-0.1251(3)	0.1350(2)	0.2631(4)	4.3(2)	4.8(3)	8.3(3)	-0.5(2)	1.7(2)	0.9(3)
C(6)	-0.1817(3)	0.1491(2)	0.1863(5)	4.3(3)	7.1(4)	11.6(4)	-0.3(2)	0.9(3)	0.6(3)
C(7)	-0.0364(2)	0.2171(2)	0.2020(4)	3.9(2)	3.9(3)	5.9(3)	-0.2(2)	1.2(2)	-0.2(2)
C(8)	-0.0606(3)	0.2483(2)	0.2786(5)	11.1(4)	4.0(3)	9.8(4)	-0.1(3)	5.5(3)	-0.9(3)
C(9)	-0.0636(4)	0.2983(3)	0.2627(7)	13.1(5)	5.7(5)	14.1(6)	0.9(4)	5.9(5)	-1.1(4)
C(10)	-0.0431(4)	0.3190(2)	0.1734(8)	9.0(4)	3.7(4)	14.6(6)	0.4(3)	1.3(4)	0.0(4)
C(11)	-0.0195(3)	0.2894(3)	0.0979(5)	8.3(4)	6.3(4)	9.4(4)	-0.3(3)	0.5(3)	3.0(4)
C(12)	-0.0164(3)	0.2374(2)	0.1115(4)	6.3(3)	4.1(3)	6.5(3)	-0.1(2)	0.6(2)	-0.1(2)
C(13)	0.0238(3)	0.1421(2)	0.3322(3)	5.2(3)	5.3(3)	4.5(2)	0.2(3)	0.6(2)	-1.1(2)
C(14)	0.0174(3)	0.1004(2)	0.3919(5)	7.7(3)	6.2(4)	7.3(3)	1.7(3)	-1.4(3)	0.0(3)
C(15)	0.0663(5)	0.0913(3)	0.4697(6)	10.8(5)	10.6(6)	7.5(4)	4.5(5)	-0.9(4)	1.1(4)
C(16)	0.1220(5)	0.1227(5)	0.4875(6)	6.8(5)	21.2(11)	5.9(4)	3.4(6)	-0.9(4)	-2.4(5)
C(17)	0.1308(4)	0.1635(4)	0.4290(6)	6.6(4)	20.0(9)	5.6(4)	-2.7(5)	0.2(3)	-2.5(4)
C(18)	0.0819(3)	0.1736(3)	0.3523(4)	6.1(3)	11.5(5)	5.3(3)	-2.4(3)	1.0(3)	-1.4(3)
C(19)	0.1552(3)	0.0923(2)	-0.1170(4)	5.9(3)	6.4(3)	5.6(3)	-1.4(2)	0.5(2)	-1.4(2)
C(20)	0.1075(3)	0.1231(3)	-0.1846(4)	9.1(4)	11.8(5)	5.6(3)	-0.2(4)	-0.6(3)	0.4(3)
C(21)	0.1935(2)	0.1681(2)	0.0279(4)	3.8(2)	4.2(3)	5.1(2)	0.4(2)	0.0(2)	0.2(2)
C(22)	0.1758(3)	0.1994(2)	0.1055(4)	6.7(3)	5.3(3)	7.0(3)	-1.6(3)	0.5(2)	-0.4(3)
C(23)	0.2126(4)	0.2434(3)	0.1233(5)	9.0(4)	5.7(4)	9.0(4)	-1.4(3)	-1.3(3)	-1.2(3)
C(24)	0.2681(4)	0.2564(2)	0.0610(8)	6.4(4)	4.1(4)	14.2(6)	-1.2(3)	-3.0(4)	1.2(4)
C(25)	0.2864(3)	0.2263(3)	-0.0156(7)	6.6(4)	5.9(4)	16.4(7)	-1.3(3)	3.0(4)	1.3(4)
C(26)	0.2497(3)	0.1824(2)	-0.0333(5)	7.4(3)	4.6(3)	11.2(4)	-1.5(3)	3.5(3)	-0.9(3)
C(27)	0.2052(2)	0.0678(2)	0.0871(4)	4.4(2)	3.3(2)	6.5(3)	-0.3(2)	-0.7(2)	-0.5(2)
C(28)	0.1907(3)	0.0593(2)	0.1884(4)	5.5(3)	6.0(3)	6.6(3)	-1.4(3)	-0.9(3)	1.4(3)
C(29)	0.2368(5)	0.0296(3)	0.2456(5)	8.1(4)	8.4(4)	9.7(4)	-3.4(4)	-2.3(4)	4.2(4)
C(30)	0.2968(4)	0.0089(2)	0.2014(9)	7.3(4)	5.0(4)	15.9(7)	-2.0(3)	-4.3(5)	5.2(4)
C(31)	0.3107(4)	0.0175(3)	0.1025(8)	6.9(4)	5.1(4)	15.1(6)	2.1(3)	-1.0(4)	1.1(4)
C(32)	0.2666(3)	0.0462(2)	0.0452(4)	6.1(3)	5.2(3)	8.8(3)	1.7(3)	-0.2(3)	0.1(3)
H(1)	-0.0750	0.2344	0.3419	8.300					
H(2)	-0.0801	0.3195	0.3153	10.830					
H(3)	-0.0453	0.3539	0.1634	9.080					
H(4)	-0.0053	0.3042	0.0353	7.990					
H(5)	-0.000	0.216	0.0586	5.620					
H(6)	-0.0219	0.0784	0.3788	7.060					
H(7)	0.0606	0.0626	0.511	9.650					
H(8)	0.1549	0.1154	0.5408	11.280					
H(9)	0.1704	0.1849	0.442	10.540					
H(10)	0.0877	0.2025	0.3118	7.590					
H(11)	-0.1346	0.1523	0.3246	5.780					
H(12)	-0.1278	0.1002	0.2748	5.780					
H(13)	-0.2284	0.1405	0.2115	7.630					
H(14)	-0.1730	0.1318	0.1245	7.630					
H(15)	-0.1797	0.1839	0.1743	7.630					
H(16)	0.1366	0.1899	0.1485	6.360					
H(17)	0.1996	0.2647	0.1779	7.890					
H(18)	0.2936	0.2866	0.0725	8.230					
H(19)	0.3256	0.236	-0.058	9.550					
H(20)	0.2629	0.1613	-0.088	7.750					
H(21)	0.1490	0.0739	0.2186	6.030					
H(22)	0.227	0.0236	0.3153	8.660					
H(23)	0.3288	-0.0114	0.2392	9.300					
H(24)	0.3525	0.0032	0.0719	9.010					
H(25)	0.2772	0.0519	-0.0246	6.640					
H(26)	0.1424	0.0583	-0.1249	5.940					
H(27)	0.2043	0.0969	-0.137	5.940					
H(28)	0.114	0.113	-0.2533	8.810					
H(29)	0.1202	0.1572	-0.1778	8.810					
H(30)	0.0583	0.1185	-0.1656	8.810					

[a] The form of the temperature factor (B in units of Å^2) is $T = \exp[-0.25(B_{11}h^2a^{*2} + B_{22}k^2b^{*2} + B_{33}l^2c^{*2} + 2B_{12}hka^*b^* + 2B_{13}hla^*c^* + 2B_{23}klb^*c^*)]$ for anisotropic parameters and $T = \exp[-B(\sin^2\theta)/\lambda^2]$ for isotropic thermal parameters.

in the Ag–P bond and, therefore, the magnitude of the P–Ag–P angle. Recently Davis et al.[2] and Lippard and Mayerle[3] suggested that the P–Cu–P angle in the $(Ph_3P)_2CuL$ complexes is significantly affected by steric factors which arise from interactions between the substituted phosphine groups and the anion (L). As part of our studies concerning the synthesis of polynuclear coordination compounds[4] we have determined the solid-state structures of several $[(Ph_3P)_2Ag]_nL$ complexes.[5,6] With $L = Ni(S_2C_2(CN)_2)_2^{2-}$, $n = 2$, various substituted phosphine analogues can be prepared. In order to obtain additional information on the factors that determine the geometry of the $Ag(PR_3)_2^+$ moiety and particularly to ascertain the relative importance of steric interactions between various phosphines and the same anion we have determined the crystal structure of the $[(EtPh_2P)_2Ag]_2Ni(mnt)_2$ complex[7] and examined the ^{31}P NMR spectra of the $[(Et_nPh_{3-n})_2Ag]_2Ni(mnt)_2$ complexes ($n = 0, 1, 2, 3$).

Experimental Section

NMR Measurements. The ^{31}P spectra were obtained on a Bruker HX90E, equipped with a broad-band proton decoupler, an SXP high-power radiofrequency amplifier, and a B-NC 12 computer. The radiofrequency applied was 36.44 MHz. The solvent was a mixture of dichloromethane–toluene-d_8 (4:1 v/v). A capillary containing 85% H_3PO_4 was used as external reference.

X-Ray Diffraction Measurements. Collection and Reduction of Data. Suitable crystals of $[Ag(PPh_2Et)_2]_2Ni(mnt)_2$[7] were obtained[8] by the slow diffusion of ether into a dichloromethane solution of the complex.

Preliminary precession photographs of the bright red, truncated octahedral crystals indicated Laue symmetry *mmm*. The systematic absences *h0l* ($l \neq 2n$), *hk0* ($h \neq 2n$), and *0kl* ($k \neq 2n$) were consistent

Table II. Intramolecular Bond Distances and Angles for $[Ag(PPh_2Et)_2]_2Ni(mnt)_2$[a]

A. Bond Lengths, Å

Ni-S(1)	2.176 (2)	Ag-S(1)	2.931 (2)
Ni-S(2)	2.177 (1)	Ag-S(2)′	2.778 (1)
Ni-Ag	2.986 (1)	Ag-P(1)	2.459 (2)
		Ag-P(2)	2.439 (2)
C(1)-S(1)	1.724 (5)		
C(1)-C(2)	1.426 (8)	P(1)-C(5)	1.835 (5)
C(1)-C(3)	1.362 (6)	P(1)-C(7)	1.815 (5)
C(2)-N(1)	1.144 (6)	P(1)-C(13)	1.815 (5)
C(3)-S(2)	1.732 (5)	P(2)-C(19)	1.811 (5)
C(3)-C(4)	1.434 (8)	P(2)-C(21)	1.818 (5)
C(4)-N(2)	1.145 (6)	P(2)-C(23)	1.813 (5)
S(1)-S(2)	3.144 (2)		
S(1)-S(2)′	3.012 (2)		
C(5)-C(6)	1.502 (7)	C(19)-C(20)	1.500 (8)
C(7)-C(8)	1.385 (7)	C(21)-C(22)	1.363 (6)
C(8)-C(9)	1.361 (8)	C(22)-C(23)	1.384 (8)
C(9)-C(10)	1.352 (10)	C(23)-C(24)	1.356 (9)
C(10)-C(11)	1.344 (9)	C(24)-C(25)	1.335 (9)
C(11)-C(12)	1.411 (8)	C(25)-C(26)	1.380 (9)
C(12)-C(7)	1.361 (6)	C(26)-C(21)	1.367 (6)
C(13)-C(14)	1.373 (7)	C(27)-C(28)	1.377 (6)
C(14)-C(15)	1.386 (9)	C(28)-C(29)	1.386 (9)
C(15)-C(16)	1.348 (11)	C(29)-C(30)	1.368 (10)
C(16)-C(17)	1.350 (12)	C(30)-C(31)	1.346 (9)
C(17)-C(18)	1.379 (10)	C(31)-C(32)	1.351 (8)
C(18)-C(13)	1.390 (7)	C(32)-C(27)	1.386 (7)

B. Bond Angles, Deg

S(1)-Ni-S(2)	92.45 (6)	Ag-P(1)-C(5)	119.7 (2)
S(1)-Ni-S(2)′	87.55 (5)	Ag-P(1)-C(7)	115.8 (2)
		Ag-P(1)-C(13)	107.1 (1)
S(1)-Ag-S(2)′	63.61 (4)	C(5)-P(1)-C(7)	103.3 (3)
S(1)-Ag-P(1)	97.16 (5)	C(5)-P(1)-C(13)	105.0 (3)
S(1)-Ag-P(2)	111.72 (5)	C(7)-P(1)-C(13)	104.5 (3)
S′(2)-Ag-P(1)	104.06 (5)		
S′(2)-Ag-P(2)	127.20 (6)	Ag-P(2)-C(19)	114.3 (2)
P(1)-Ag-P(2)	128.00 (6)	Ag-P(2)-C(21)	118.7 (2)
Ni-Ag-P(1)	133.78 (3)	Ag-P(2)-C(27)	109.1 (2)
Ni-Ag-P(2)	94.09 (3)	C(19)-P(2)-C(21)	105.0 (3)
Ni-Ag-S(1)	43.14 (4)	C(19)-P(2)-C(27)	107.0 (3)
Ni-Ag-S′(2)	44.20 (3)	C(21)-P(2)-C(27)	101.6 (2)
C(1)-S(1)-Ni	102.6 (2)	C(1)-C(2)-N(1)	178.4 (7)
C(3)-S(2)-Ni	102.8 (2)	S(2)-C(3)-C(4)	117.2 (3)
S(1)-C(1)-C(2)	117.3 (3)	S(2)-C(3)-C(1)	120.4 (3)
S(1)-C(1)-C(3)	121.6 (3)	C(1)-C(3)-C(4)	122.3 (5)
C(2)-C(1)-C(3)	121.1 (5)	C(3)-C(4)-N(2)	178.0 (6)

only with the orthorhombic space group *Pbca* (No. 61).

A crystal of approximate dimensions 0.29 × 0.32 × 0.31 mm was mounted on a glass fiber in air and aligned on a Picker-Nuclear four-circle diffractometer, equipped with a scintillation counter and pulse height analyzer and automated by a DEC PDP8-I and FACS-I DOS software. Graphite-monochromatized molybdenum radiation was used throughout (λ(Mo Kᾱ) 0.7107 Å, $2\theta_m$ = 12.50°). Accurate cell dimensions were determined by least-squares refinement on the 2θ values of 12 carefully centered reflections which yielded a = 18.427 (9) Å, b = 26.894 (10) Å, and c = 13.149 (9) Å at 24 °C. The calculated density of 1.44 g cm^{-3} for Z = 4 agrees well with the pycnometrically determined density of 1.42 (2) g cm^{-3}. Two octants of intensity data ($+H$, $\pm K$, $+L$) were collected for $0° \leq 2\theta \leq 40°$ using a θ–2θ scan technique. Peaks were scanned at 1.0°/min from 0.5° below the predicted $K\alpha_1$ position to 0.5° above the predicted $K\alpha_2$ position. Background intensities were counted for 10 s at each end of the scan. Zirconium attenuators were automatically inserted in the diffracted beam whenever the count rate exceeded 10000 counts/s, and the peak and background were remeasured with the attenuators in place. Three reflections (704, $\bar{4}04$, 0, 14, 0) were measured after every 100 data points to monitor crystal and apparatus stability. No systematic trends in the intensities of the standards were observed throughout the data collection period. A total of 6014 nonextinct reflections were measured. Net intensities and their standard deviations were calculated, Lorentz and polarization factors were applied, and equivalent reflections were averaged, as described previously,[6] to give 3049 unique reflections. Of these 2118 had $F^2 > 3\sigma(F^2)$. No absorption correction was applied to the data (μ = 11.3 cm^{-1}). The scattering factors of Doyle and Turner[9] were used for the neutral atoms except hydrogen, together with the real and imaginary dispension terms of Cromer and Liberman.[10] The spherical hydrogen scattering factors of Stewart, Davidson, and Simpson were used.[11] Least-squares procedures and the weighting scheme have been described previously.[6] Zero weights were assigned to reflections with $F^2 < 3\sigma(F^2)$, and $1/\sigma^2(F)$ was assigned to all others. The uncertainty parameter, p, was 0.04 throughout the refinement.

Table III. $Ag(PPh_2Et)_2$–$Ni(mnt)_2$ Contacts ≤3.60 Å

C(28)-C(1)	3.438 (7)	C(32)[b]-N(1)	3.374 (8)
C(29)-C(2)	3.587 (8)	C(31)[b]-N(1)	3.421 (11)
C(15)[a]-N(1)	3.548 (11)		

[a] $-x, -y, 1-z$. [b] $1/2 - x, -y, 1/2 + z$.

Table IV. Weighted Least-Squares Planes and Dihedral Angles

Deviations from the Planes (Å) of Atoms Used to Define the Planes

Atom	Plane 1	Plane 2	Atom	Plane 1
Ag		0.000	C(1)	0.006 (5)
Ni	0.011 (0)	−1.04	C(2)	0.022 (6)
S(1)	−0.0019 (13)		C(3)	−0.009 (5)
S(2)	0.0019 (13)		C(4)	−0.002 (6)
P(1)		0.000	N(1)	0.017 (6)
P(2)		0.000	N(2)	−0.023 (5)

Dihedral Angles between Selected Planes, Deg

Plane 1–plane 3[a]	−0.44	Plane 1–plane 10[d]	−15.40
Plane 1–plane 8[b]	10.81	Plane 2–plane 3	−69.90
Plane 1–plane 9[c]	−89.05	Plane 3–plane 4[e]	−85.83

[a] Plane 3 is Ni-S(1)-S(2). [b] Plane 8 is P(2)-C(19)-C(20). [c] Plane 9 is the phenyl ring on P(2), C(21)–C(26). [d] Plane 10 is the phenyl ring on P(2), C(27)–C(32). [e] Plane 4 is Ag-S(1)-S(2)′.

Solution and Refinement of the Structure. With Z = 4 in the eightfold space group *Pbca* the nickel is required to occupy a center of symmetry. The position of the silver atom was determined from the three-dimensional Patterson map and both the Ni (at 0, 0, 0) and the Ag atoms were used to phase the first Fourier synthesis. Successive cycles of least-squares calculations followed by Fourier syntheses revealed the rest of the structure. With isotropic thermal parameters for all atoms the refinement converged at $R_1 = \sum||\Delta F|/\sum|F| = 0.081$. Thhe Ni, the Ag, and the two P atoms and the atoms in the mnt ligand were then allowed to refine with anisotropic thermal parameters to an R value of 0.052. At this stage the hydrogen atoms were included at calculated positions (d(C–H) = 0.95 Å) but not refined. This reduced the R value to 0.044. The rest of the nonhydrogen atoms were allowed to refine anisotropically. Hydrogen atom positions were calculated after each cycle and their isotropic thermal parameters were set equal to those of the carbons to which they were attached. In the final cycle of least squares all parameter shifts were less than their esd from the inverse matrix and most were less than 0.1σ. The R_1 value after the last cycle was 0.023 and R_2 ($\sum w(\Delta F)^2/\sum wF^2$) was 0.027 for 358 parameters on 2113 data. The standard deviation of an observation of unit weight was 0.83.

Results and Discussion[12]

Atomic positional parameters with standard deviations are compiled in Table I. Intramolecular bond distances and angles are given in Tables II and III. The atom labeling scheme is shown in Figure 1, and a stereodrawing in Figure 2.

The coordination geometries about the silver and nickel atoms in the present structure are similar to those observed in the structures of the $[(PPh_3)_2Ag]_2Ni(mnt)_2$ and $[(PPh_3)_2Ag]_2Ni(i\text{-}mnt)_2$ complexes.[5] The molecule has a crystallographic center of symmetry so that the coordination around the nickel is rigorously planar and the Ag–Ni–Ag angle rigorously 180°. The nickel is coordinated by the four sulfur atoms of the mnt ligands. The silver atom is approximately trigonally hydridized and forms two "normal" Ag–P bonds;

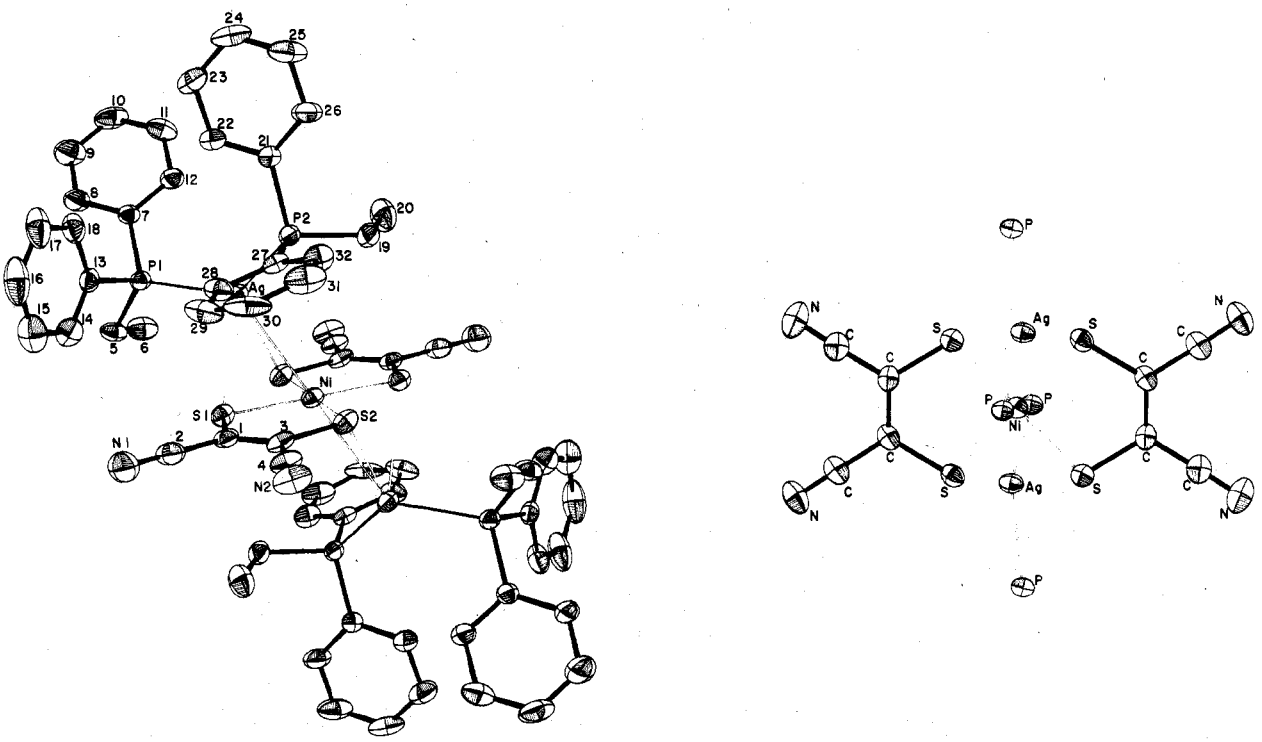

Figure 1. Structure of $[Ag(PPh_2Et)_2]_2Ni(mnt)_2$. Thermal vibrational ellipsoids are scaled to enclose 50% probability.

Table V. NMR and Conductivity Data for the $(PR_3)_2AgL$ Complexes

Compd[a]	Equiv conductance, Ω^{-1} cm^2 equiv^{-1} (in CH_2Cl_2, 10^{-2} M at 195 K)	$J_{^{107}Ag-P}$ ($J_{^{108}Ag-P}$), Hz[b]	P-Ag-P, deg	Ag-P, Å	Rate, s^{-1} (Temp, K)[c]
$(PPh_3)_2AgL$	0.17	394 (451)	118.5 (1)	2.504 (4) 2.465 (3)	7789 (298) 4209 (290) 917 (273) 231 (257)[e]
$(PEtPh_2)_2AgL$	0.05	413 (475)	128.00 (6)	2.459 (2) 2.439 (2)	5646 (298) 3239 (290) 923 (273) 268 (257)[e]
$(PEt_2Ph)_2AgL$	Nil	426 (489)			1145 (298) 513 (290)[e]
$(PEt_3)_2AgL$	Nil	426 (489)			403 (298) 255 (290) 89 (273) 58 (265)[e]
$(P(tol)_3)_2AgF$[d]		450			
$(P(tol)_3)_2AgCl$[d]		378			3612 (228)[d]
$(P(tol)_3)_2AgCN$[d]		278			
$(P(tol)_3)_2AgNO_3$[d]		470			4478 (283)[d]
$(P(tol)_3)_2AgPF_6$[d]	14.0	496			4400 (293)[d]

[a] Ph = C_6H_5, Et = C_2H_5, tol = C_7H_8, L = bis(1,2-dicyano-1,2-ethylenedithiolato)nickel(II), $Ni(mnt)_2^{2-}$. [b] Parameters obtained at 232 K; accuracy of the measurements ±1 Hz. [c] Based on line shape analysis of NMR data. [d] From ref 1. [e] E_a for dissociation of phosphine is 13.5 ± 1, 11.5 ± 1, 11 ± 2, and 10 ± 1 kcal/mol for compounds 1–4, respectively; accuracy of the temperature in parentheses ±3 K.

the remaining hybrid orbital on the silver is oriented toward the centroid of a triad of atoms defined by the nickel atom and two sulfurs (Figure 1).

The observed Ag–S and Ag–Ni distances (Table II) are longer than single covalent bonds but appreciably shorter than the van der Waals contacts of 3.52 and 3.35 Å for Ag–S and Ag–Ni, respectively.[13] The distance of the silver atom from the centroid of the Ni–S(1)–S(2) triad (Figure 1) is 2.520 Å and is slightly greater than the analogous distances calculated for the $Ag(PPh_3)_2^+$ adducts of $Ni(mnt)_2^{2-}$ and $Ni(i\text{-}mnt)_2^{2-}$ (2.468 and 2.408 Å, respectively). The primary differences between this structure and that of the PPh_3 analogue are in the conformation of the diphenylethylphosphine, as compared to the triphenylphosphine, and in the size of the P–Ag–P angle.

The striking feature of the orientation of the phosphines is the formation of planes of atoms above and below the Ni(mnt)$_2$ plane. The phenyl ring that contains C(27)–C(32) forms a dihedral angle of only 15.4° with the mnt plane, and the P(2)–C(19)–C(20) plane forms an angle of only 10.8° with the mnt plane (Table III, Figure 2). There exist very short intramolecular contacts between one of the phenyl rings and the mnt ligand. Those between C(32) and N(1) of 3.374 (8) Å and between C(31) and N(1) of 3.421 (11) Å are outstanding with several other contacts ≤3.50 Å (Table IV).

The P–Ag–P angle of 128° is 10° larger than the corresponding angle in $[(PPh_3)_2Ag]_2Ni(mnt)_2$. This ability of the P–Ag–P angle to open up, optimizing the contacts between the phosphine and the mnt ligand, is clearly due to the reduced

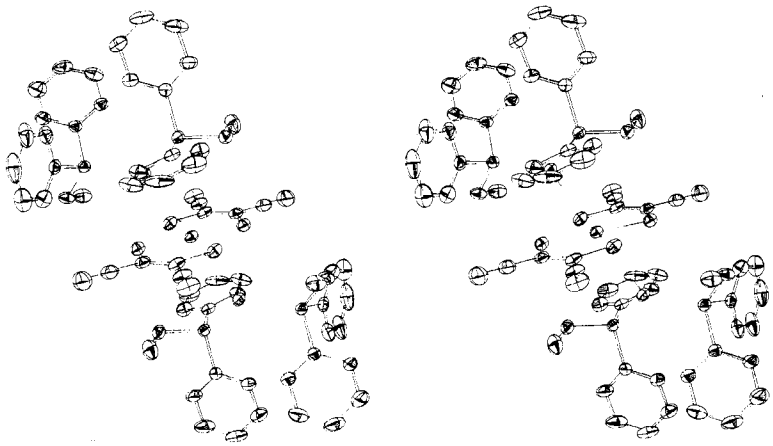

Figure 2. Stereoscopic view of $[Ag(PPh_2Et)_2]_2Ni(mnt)_2$.

Table VI

	P-Ag-P, deg	Av Ag-P, Å	Ag-NiS_2 (centroid), Å
$[(PPh_3)_2Ag]_2Ni(mnt)_2$	118.5	2.484	2.468
$[(EtPh_2P)_2Ag]Ni(mnt)_2$	128.0	2.449	2.520

steric hindrance of the ethyl group vs. a phenyl group. A phenyl group lying in the same plane as P(2)–C(19)–C(20) would interact strongly with the C(27)–C(32) phenyl group and upon rotation around the P–C bond would interfere strongly with the mnt ligand.

The ^{31}P NMR spectra were examined for various substituted phosphine complexes of the type $[Ag(PR_3)_2]_2Ni(mnt)_2$. The magnitudes of the Ag–P coupling constants (Table V) increase in the order $PPh_3 < PEtPh_2 < PEt_2Ph = PEt_3$. This increase in J_{Ag-P} may be interpreted as a consequence of reduced steric strain which allows the P–Ag–P angle to open and the s character of the P–Ag bond to increase from PPh_3 to PEt_3. Alternatively the increase in s character of the P–Ag bond, reflected in the magnitude of the coupling constants,[14] may arise because of the increased basicity of the phosphines upon the successive introduction of alkyl groups. A summary of the Ag–P bond lengths, the Ag–NiS_2 "centroid" distances, and the P–Ag–P angles of stuctures, in which *similar bonding interactions occur*, is presented in Table VI.

Slightly shorter Ag–P bonds and slightly longer Ag–NiS_2 "centroid" distances are observed as the P–Ag–P angle increases. These observations are in accord with the expectation that an increase of the s character in the Ag hybrid orbitals will be accompanied by a slight decrease in the electrophilic nature of the Ag atom. Although it could be argued that a decrease in the Ag–NiS_2 interaction might result in a larger P–Ag–P angle, the NMR and structural data suggest that steric effects are important on the basis of the following considerations: (a) To the extent that the electronic effects of alkyl substituents are additive[15,16] one might expect a proportional change in the magnitude of J_{Ag-P} between the PEt_2Ph and PEt_3 compounds. In fact, the values for these two complexes are identical. (b) Substitution of a phenyl by an ethyl group in PPh_3 relieves *some* of the strain as shown by a comparison of the present structure to the PPh_3 analogue. However, appreciable steric hindrance is still in evidence in the present structure.

The NMR data show that there exists a difference in the Ag–P coupling constants between the PEt_2Ph and $PEtPh_2$ derivatives. No such difference is found between PEt_2Ph and PEt_3. These results indicate that the values for J_{Ag-P} and indirectly the magnitudes of the P–Ag–P angle and the percent s character in the P–Ag bond are affected by $Ag(PR_3)_2^+$–mnt steric interactions.

Acknowledgment. The authors wish to thank the National Science Foundation for Grant GP 28567, which partially supported this research. D.C. is grateful to the Alfred P. Sloan Foundation for a fellowship, 1972–1974.

Registry No. $[(PEtPh_2)_2Ag]_2$, 59654-43-2; $[(PPh_3)_2Ag]_2$, 50860-39-4; $[(PEt_2Ph)_2Ag]_2$, 59654-45-4; $[(PEt_3)_2Ag]_2$, 59654-47-6; $(P(tol)_3)_2AgF$, 59654-48-7; $(P(tol)_3)_2AgCl$, 29115-60-4; $(P(tol)_3)_2AgCN$, 29062-74-6; ^{31}P, 7723-14-0.

Supplementary Material Available: Compilation of observed structure factor amplitudes, their estimated standard deviations, and the difference $|F_o| - |F_c|$ (12 pages). Ordering information is given on any current masthead page.

References and Notes

(1) E. L. Muetterties and C. W. Alegranti, *J. Am. Chem. Soc.*, **94**, 6386 (1972).
(2) P. H. Davis, R. L. Bedford, and I. C. Paul, *Inorg. Chem.*, **12**, 213 (1973).
(3) S. J. Lippard and J. J. Mayerle, *Inorg. Chem.*, **11**, 753 (1972).
(4) M. L. Caffery and D. Coucouvanis, *J. Inorg. Nucl. Chem.*, **37**, 2081 (1975).
(5) F. J. Hollander and D. Coucouvanis, *Inorg. Chem.*, **13**, 2381 (1974).
(6) D. Coucouvanis, N. C. Baenziger, and S. M. Johnson, *Inorg. Chem.*, **13**, 1191 (1974).
(7) The following abbreviations will be used throughout the text: mnt, 1,2-dicyano-1,2-ethylenedithiolate; *i*-mnt, 1,1-dicyano-1,1-ethylenedithiolate; PPh_3, triphenylphosphine; Et, ethyl.
(8) The synthesis of this complex and of the corresponding $PPhEt_2$ and PEt_3 analogues which were prepared in analytically pure form was accomplished by procedures outlined in ref 4 under a nitrogen atmosphere.
(9) P. A. Doyle and P. S. Turner, *Acta Crystallogr., Sect. A*, **24**, 390 (1968).
(10) D. T. Comer and D. Liberman, *J. Chem. Phys.*, **53**, 1891 (1970).
(11) R. F. Stewart, E. R. Davidson, and W. T. Simpson, *J. Chem. Phys.*, **42**, 3175 (1965).
(12) Supplementary material available.
(13) For further discussion of the Ag–S and Ag–P bond lengths see ref 5.
(14) For comments concerning the validity and limitations in correlations of J_{Ag-P} vs. s character of the Ag–P bond see footnote 17 in ref 1.
(15) W. A. Henderson and C. A. Streuli, *J. Am. Chem. Soc.*, **82**, 5791 (1960).
(16) W. A. Henderson and S. A. Buckler, *J. Am. chem. Soc.*, **82**, 5794 (1960).